NACA TN 2458

NATIONAL ADVISORY COMMITTEE FOR AERONAUTICS

TECHNICAL NOTE 2458

AN INSTRUMENT EMPLOYING A CORONAL DISCHARGE FOR THE DETERMINATION OF DROPLET-SIZE DISTRIBUTION IN CLOUDS

By Rinaldo J. Brun, Joseph Levine, and Kenneth S. Kleinknecht

Lewis Flight Propulsion Laboratory
Cleveland, Ohio

Washington

September 1951

NATIONAL ADVISORY COMMITTEE FOR AERONAUTICS

TECHNICAL NOTE 2458

AN INSTRUMENT EMPLOYING A CORONAL DISCHARGE FOR THE DETERMINATION OF DROPLET-SIZE DISTRIBUTION IN CLOUDS

By Rinaldo J. Brun, Joseph Levine, and Kenneth S. Kleinknecht

SUMMARY

A flight instrument that uses electric means for measuring the droplet-size distribution in above-freezing clouds has been devised and given preliminary evaluation in flight. An electric charge is placed on the droplets and they are separated aerodynamically according to their mass. Because the charge placed on the droplets is a function of the droplet size, the size spectrum can be determined by measurement of the charge deposited on cylinders of several different sizes placed to intercept the charged droplets. An expression for the rate of charge acquisition by a water droplet in a field of coronal discharge is derived. The results obtained in flight with an instrument based on the method described indicate that continuous records of droplet-size spectrum variations in clouds can be obtained. The experimental instrument was used to evaluate the method and was not refined to the extent necessary for obtaining conclusive meteorological data.

The desirable features of an instrument based on the method described are (1) The instrument can be used in clouds with temperatures above freezing; (2) the size and the shape of the cylinders do not change during the exposure time; (3) the readings are instantaneous and continuous; (4) the available sensitivity permits the study of variations in cloud structures of less than 200 feet in extent.

INTRODUCTION

In the problem of all-weather flying, the physics of clouds is of great importance because clouds can cause aircraft icing, interference with radar, turbulence, and limitations of visibility. The necessity for a knowledge of the physical characteristics of the icing cloud is evident when the fundamental variables that determine the areas of impingement of freezing cloud droplets on aircraft parts are examined.

The rotating-multicylinder method described in references 1 and 2 has been used to measure liquid-water content and droplet-size distribution in icing clouds. The operation of this method is based on the

principle that when cylinders of various diameters are moved through a cloud, the amount of water intercepted per unit projected area of each cylinder is dependent on the diameter of the cylinder and the inertia of the cloud droplets. Those supercooled droplets that strike the cylinders freeze onto the cylinders. The collection efficiency of cylinders, defined as the ratio of the amount of water intercepted to the amount of water originally contained in the volume swept out by the cylinders, has been calculated (reference 1) and is a known function of drop diameter, cylinder diameter, airspeed, temperature, and pressure. Collection efficiency is an increasing function with increasing droplet diameter, decreasing cylinder diameter, and increasing airspeed. From these known relations, the liquid-water content, the volume-median drop diameter[1], and the drop size distribution can be calculated from the weights of ice collected during the simultaneous exposure of several cylinders of different diameters.

Data obtained by the rotating-multicylinder method have been valuable in computations for the design of thermal ice-prevention systems. The cylinders collect ice in a manner similar to that of airplane components; therefore, the intrinsic value of the method should not be underestimated. There are limitations, however, to the rotating-multicylinder method in the study of cloud physics. An important phase in the study of the formation of clouds is the investigation of the drop size and drop-size distribution in clouds above the freezing temperature. A knowledge of the conditions in clouds above the freezing temperature is also necessary for the study of turbulence and atmospheric forecasting.

A method that permits the study of the continuous variations in the structure of clouds having temperatures above freezing has been devised and given preliminary evaluation in flight at the NACA Lewis laboratory. The method is based on the principle that an electric charge of known quantity can be placed on each droplet in a sample of the cloud. Because the amount of electric charge placed on the droplets is a function of their size, their mass can be measured electrically. The droplets in the cloud sample are charged by a coronal discharge taking place between two plates oriented parallel to an airstream. After the droplets are charged, they are separated according to their size. The method of separation involves the use of cylinders of various sizes placed in the path of the droplets. As with the rotating-cylinder method, collection efficiencies of the cylinders of different sizes are functions of drop size and cylinder

---

[1]The amount of water in all the drops of a diameter greater than the volume-median drop diameter is equal to the amount of water in all the drops of smaller diameter. Volume-median drop diameter is often referred to as "mean-effective drop diameter."

diameter. The charge deposited on each cylinder represents a measure of the total number of droplets intercepted. The rate of water interception by the cylinders is measured in terms of an electric current rather than in the form of deposited ice, as in the case of the rotating-cylinder method.

An instrument employing the method described was constructed and attached to the under side of a light-bomber-type airplane. Records were obtained of the droplet-size variations in flights through various types of cloud in order to prove the method feasible. All the clouds were above the normal freezing temperature.

A part of the method presented in this report has appeared in a dissertation titled "Some Aspects of Aircraft Icing Problem and an Instrument for Its Study" by Rinaldo J. Brun presented to the faculty of the Yale School of Engineering in June 1949 in candidacy for the degree of Doctor of Engineering.

SYMBOLS

The following symbols are used herein. (All electrical units are in electrostatic units in the cgs system.)

A,B,C	arbitrary constants to be evaluated according to boundary conditions
a_0	volume-median droplet radius, centimeters
E_c	electrical collection efficiency of cylinders
E_M	mass collection efficiency of cylinders
E_r	radial component of electric field strength
E_x	x-component of electric field strength
E_0	undisturbed electric field strength
F_r	radial force of attraction between electron and droplet, dynes
j	current density in ionized field
K	droplet-inertia parameter
k	electron ion mobility

L	significant dimension of obstacle, centimeters
l	distance between anode and needle points, centimeters
m	mass of droplet, grams
N	total number of droplets in volume swept out by cylinder
N_i	number of droplets of group size i that impinge on cylinder
Q	charge on droplet
Q_∞	saturation charge on droplet
r	radial distance from center of droplet to electron, centimeters
t	time interval during which droplet is being charged, seconds
U	free-stream velocity, centimeters per second
V	electrostatic potential at any point in field
V_t	electrostatic potential applied to cathode
v_x	x-component of droplet velocity, centimeters per second
x,y,z	rectangular coordinates
Y	length of cathode, centimeters
Y_s	length of sweepout field, centimeters
ϵ	electron charge
θ	angle between radial force component of electron attraction to droplet and x-axis through center of droplet, radians
θ_0	terminating angle of approach of electrons to droplet, radians
λ	thickness of luminous layer
μ	viscosity of air, grams per second per centimeter
ν	distance from surface of droplet to electron, as fractional part of radius

ρ charge density in ionized field

ρ_a density of air, grams per cubic centimeter

ρ_w density of water droplet, grams per cubic centimeter

σ specific inductive capacitance

τ ratio of electrical charge contained in particular group in question compared with total of charge contained in all groups

Φ dimensionless parameter defined by equation (C1)

ψ force-field function

ω radius of tube of force lines

PRINCIPLE OF OPERATION

A method for measuring cloud-droplet size is presented. An electrical charge is placed on the droplets and they are aerodynamically separated according to their mass. A system for charging cloud droplets is schematically shown in figure 1. The system consists of two parallel plates designated A and C. A coronal discharge exists between the plates along the distance indicated by Y. Cloud droplets enter the region of coronal discharge in the direction of the air velocity and acquire a charge while they are in the region of coronal discharge. After leaving the region of coronal discharge, the droplets follow paths governed by the air flow around obstacles placed beyond the parallel plates. Cylinders of various sizes are considered practical obstacles because the droplet impingement on cylinders is known, as described in references 1 and 2. Upon striking the cylinders the droplets leave their charge on the cylinder surface. The rate of charge deposit is measured by a microammeter placed in the circuit as shown in figure 1 or by a recording galvanometer. The current readings from several different sizes of cylinders can be translated into droplet-size distribution by methods subsequently described.

Field of coronal discharge. - The coronal discharge between plates A and C (fig. 1) is induced by an electric potential produced with a high-voltage direct-current power supply. Needles, indicated by B in the figure, are inserted into the cathode plate C to aid in obtaining a uniform coronal discharge at a much lower potential drop than would be necessary with smooth parallel plates. With the existence

of a coronal discharge between the plates, a layer of luminous atmosphere is formed around the points of the needles. The luminosity extends out into the field a short distance λ (fig. 1). The luminous layer is caused by the ionization processes taking place in that region. These processes result in the formation of positive ions and negative electrons by the collision of other electrons with the air molecules. The positive ions move to the cathode plate C, which is at a high negative potential, and the electrons move to the anode plate A, which in the experiments is maintained at ground potential.

The current measured from each different size of cylinder can be translated into droplet-size distribution only if an expression is known for the rate of charge acquisition by a water droplet in a field of coronal discharge. In order to derive the expression for the rate of charge acquisition, a knowledge of the field strength and the forces of attraction between the electrons and the droplets is necessary everywhere in the field of coronal discharge.

The mechanism of the electrical discharge through gases is very well described in several textbooks (references 3 to 5). The solution of the equation for the field strength is very difficult for the complete region between two plates in which ions of more than one kind exist. In this report, a solution to the field equation is obtained that is complete enough to be of use. The solution is obtained by: (1) the use of physical conditions that best lend themselves to a solution of the equations, (2) the measurement of as many unknowns as possible, and (3) the use of reasonable simplifying assumptions.

The derivation of the expression for the electric field strength E_0 in the region of coronal discharge is given in appendix A. The equation derived is

$$E_0^2 = \frac{8\pi j x}{k} + \left(\frac{V_t}{l}\right)^2 \tag{1}$$

The assumption is made that in the region between the luminous layer and the anode plate the electrons moving toward the anode constitute the only current. Calculations employing this assumption for the case of corona in coaxial cylinders are in substantial agreement with experimental observations (references 3 and 5 to 7). For the instrument used in the tests reported herein, no serious error was made in the final results by ignoring the effect on E_0 of the current in the space between the plates and

$$E_0 = \frac{V_t}{l} \tag{2}$$

was found to be valid (appendix A).

Charging of droplet. - Equations are presented for the forces that govern the capture of an electron by a spherical water droplet placed in an ionized field, such as the field between λ and the anode in figure 1. The spherical droplet acquires a charge by its electrical attraction of the electrons. The electrons follow the lines of force that lead to the droplet, as indicated in figure 2. The droplet ceases to acquire more electrons from the field when the radial force of attraction between the electrons in the field and the droplet is zero or negative anywhere in the field for all angles of approach.

The expression for the radial component of the force exerted on an electron of charge ϵ situated at a neighboring point P a distance r from O is derived in appendix B. A conducting spherical droplet (fig. 3) of radius a with center O and with negative charge Q is considered located at a coordinate point x, where the field E_0 is determinable from equation (1) or (2). The derivation is based on the following assumptions:

1. The field strength E_0 does not vary in the neighborhood of the droplet because of space charge; that is, the droplet is located in a uniform field. The influence of the space charge on E_0 has been shown to be small (appendix A).

2. Other droplets that may be in the field are so far from the one under consideration that they do not influence the force on the electron. Under average conditions, clouds have been found to consist of droplets of 20 microns in diameter spaced approximately 100 diameters apart.

3. Other electrons surrounding the droplet do not affect the radial component of the force between the electron at P and the droplet.

4. The only charges attracted by the spherical droplet are electrons. The significant number of positive ions formed are in the luminous region λ and are swept out to the cathode. The mobility of any ion formed by molecules in the air is so much smaller than the electron mobility that the charging by large ions is of no consequence.

The radial component of force of attraction between the droplet and the negatively charged electron is

$$F_r = -\epsilon E_r = -\left[\left(1 + \frac{2a^3}{r^3}\right)\epsilon E_0 \cos\theta\right] - \frac{\epsilon Q}{r^2} - \left[-\frac{\frac{a}{r}\epsilon^2}{\left(r - \frac{a^2}{r}\right)^2} + \frac{a\epsilon^2}{r^3}\right] \quad (3)$$

The angle θ is measured counterclockwise from the x-axis to the radial-force component (fig. 3). The first bracketed term in equation (3) is the effect of a conducting spherical droplet in a uniform field caused by the field distortion in the neighborhood of the droplet; the second term is the effect of the charge Q on the droplet; and the third term (bracketed) is the effect obtained by applying Coulomb's law that the force of attraction between the electron and the ungrounded droplet is equal to that between the electron and its image.

As the charge Q acquired by the sphere increases in magnitude, the force F_r becomes zero for successively smaller values of the polar angle θ. Thus, the charge can be imagined funneled through a cone for which the half-vertex angle θ decreases as the amount of charge Q acquired by the sphere increases (fig. 2). The expression for the rate of charge acquisition by the droplet is derived in appendix B. The charge acquired as a function of time was found to be

$$Q = \left(1 + 2\,\frac{\sigma-1}{\sigma+2}\right)\frac{\pi a^2 E_0 j t}{E_0 + j\pi t} \tag{4}$$

Inasmuch as specific inductive capacitance $\sigma = 81$ for water, the effect of the specific inductive capacitance is practically negligible. The manner in which charge acquisition varies with time is shown in figure 4 for three values of j and for $E_0 = 10.92$ electrostatic units per centimeter. For large values of time t

$$Q_\infty = 3E_0 a^2 \tag{5}$$

Droplet size and collection efficiency. - The droplet size can be obtained from equation (4) when the time interval during which the droplet remains in the region of coronal discharge and the charge deposited by the droplet upon striking the cylinder are known. The time interval is obtained from a knowledge of the air-stream velocity and the physical dimension Y (fig. 1). The size and the number of droplets per unit volume of cloud are measured in terms of the current to ground from the cylinders of different sizes placed directly in the path of the droplets downstream of the coronal-discharge field. The size of the droplets impinging on the cylinders is a function of the size of the cylinders. Both the large and small droplets impinge on the very small cylinders, whereas mostly the large drops impinge on the large cylinders. A method for resolving the rate of ice accumulation on a group of different-sized cylinders into effective droplet-size distribution of a cloud is presented in reference 1. The method is essentially retained herein, but it is modified in order to translate electrical readings of the current from the cylinders into effective droplet-size distribution.

In a cloud the water drops are often not of uniform size. Five different droplet-size distribution patterns have been defined for convenience in classification of clouds (reference 1). The table of distribution patterns, reproduced herein as table I, was adapted to cover some of the probable range encountered in nature. The droplet-size ratios given in table I are the ratios of the average radius of the droplets in each subdivision to the radius a_0 of the volume-median drop size.

In order to use the work of reference 1 to translate the electrical readings into droplet-size distribution, the following expressions are derived: If, in a cloud of uniform droplet size, N_i is the number of droplets of radius a that impinge on a cylinder in a given time and N is the total number in the volume swept out by the cylinder in the same time, the electrical collection efficiency is

$$E_c = \frac{N_i Q}{NQ} = \frac{N_i}{N}$$

In this equation, E_c can also be considered as the ratio of the charge deposited on the cylinder to the total charge in the volume swept out by the cylinder. From the usual definition of collection efficiency,

$$E_M = \frac{N_i}{N} = E_c$$

in the case of uniform droplet size (distribution A, table I).

The electrical collection efficiency for distributions B, C, D, and E cannot be evaluated as readily as for A and must be computed by a rather lengthy method presented in appendix C. The droplet-size distribution is obtained by a comparison of observed data with computed values of corresponding information given in table II. The method for performing this operation is very similar to that described in references 1 and 8 for ice accretion on rotating cylinders and is briefly outlined in appendix C.

Droplet deflection. - A knowledge of the deflection of the charging droplets as they pass through the coronal field is important in order to determine the best position of the cylinders, as will be discussed in the next section. The equation of motion is written with air resistance neglected and with the provision that the x-component of the velocity obtained with this assumption will be examined to determine whether it is large enough to contribute appreciably to the air resistance.

$$m \frac{dv_x}{dt} = -Q E_0$$

$$dv_x = - \frac{3\pi {E_0}^2 a^2 j}{m} \frac{t}{\pi j t + E_0} dt$$

$$v_x = - \frac{3a^2 {E_0}^2}{m} \left[t - \frac{E_0}{\pi j} \log_e \left(\frac{\pi j t + E_0}{E_0} \right) \right] \tag{6}$$

$$x = - \frac{Q_\infty E_0}{2m} t^2 + \frac{Q_\infty {E_0}^2}{\pi j m} \left(\frac{E_0}{\pi j} + t \right) \log_e \left(1 + \frac{\pi j}{E_0} t \right) - \frac{3a^2 {E_0}^3 t}{\pi j m} + X_0 \tag{7}$$

where X_0 is the value of x when the droplet enters the ionizing field.

For $t = 0.0083$ second, which corresponds to the condition of an air-stream speed of 200 miles per hour and a coronal field 30 inches long, a droplet 10^{-3} centimeter in radius deviates by 0.98 centimeter from a straight line in passing through the coronal field ($E_0 = 10$ e.s.u./cm and $j = 10^3$ e.s.u./sq cm). The deviation is so small that very few of the droplets are deflected against the grounded plates. The velocity v_x is found to be very low (in the order of 10 ft/sec, equation (6)), so that the air resistance can be neglected in the equation of motion.

A knowledge of the deflection of the charging droplets as they pass through the coronal field is also important in order to obtain the mass of the largest particles in the atmosphere, particularly when an instrument is mounted on an airplane. In equation (7), Q_∞ can be expressed in terms of the mass of a particle. In order to obtain the mass of the largest particle in the atmosphere, the air-stream speed is decreased until no current is noted from the small cylinders. The mass of the largest particle is calculated from equation (7) by determining the trajectory of particles that enter the ionizing field near the cathode and are deflected by the electric field in the distance $Y + Y_s$ to just miss the cylinders (dashed line in fig. 1).

DESCRIPTION OF INSTRUMENT

An instrument based on the principle of operation described in the preceding section was constructed. The instrument comprised four air-stream channels back to back as shown in figure 5. Needles were inserted through the cathode plate to aid in obtaining a uniform coronal

discharge. The needles protruded through both sides of the cathode plates; thus each plate acted as a cathode for two air-stream channels. Cylinders of four different sizes were installed directly behind the region of coronal discharge (fig. 6). The assembly was hung from the under side of the fuselage of a twin-engine light-bomber-type airplane (fig. 7).

In order to obtain maximum coronal discharge in the ionizing field with the direct-current voltage supply available, the physical dimensions of an instrument must be carefully considered. The distance l from the needle points to the grounded anode was experimentally determined by constructing a laboratory model in which the current density was observed when l was varied. A value of 7.5 centimeters was determined to be the largest consistent with steady coronal discharge for the direct-current potential of 25,000 volts available to apply across the plates. The adjustment of the distance l between the cathodes and the ground plates was made with the aid of numerous plugs located to measure the current density j at various positions (fig. 6). The plugs, all of the same area, were insulated from the ground plate. The cathodes were adjusted with respect to the ground plates so that all the plugs read the same value of j.

The length Y of the coronal discharge (fig. 1) was a compromise between the amount of charge desired on a droplet and structural complications in mounting the instrument on the airplane as well as aerodynamic considerations in flight. It is desirable to charge a droplet nearly to saturation or to a state represented by points beyond the knee of the charging curves, such as point A on figure 4; errors in measuring j, and particularly in the airplane speed, which determines the time a droplet remains in the charging field, then reflect less on calculated values of Q than if the charging time were small. When the instrument is used on a modern fast-flying airplane, the length required for the desired charging time complicates the construction. In the instrument, a length Y of 30 inches was chosen to allow mounting on one of the bomb-bay doors of the light bomber.

The insulation between the cathode, which was at a high negative potential, and the ground presented some difficulties caused by moisture collection on the surfaces of the insulators. The insulators used were commercial ceramic, high-voltage transformer bushings with 3/4-inch holes through their centers. In order to avoid moisture formation on the insulator surfaces inverted cups were placed around the insulators, as shown in figure 6, to protect them from droplets that might impinge on them directly. A blanket of dry hot air bled from the thermal deicing system of the airplane was maintained inside the cups to avoid condensation on the insulator surfaces.

A gasoline-engine-driven generator furnished the 220-volt, three-phase power required to operate the high-voltage direct-current power supply. Both the engine-generator and the high-voltage power supply were mounted inside the bomb bay of the airplane. The high-voltage power supply was designed and constructed to operate at maximum voltage up to 25,000-foot altitude without internal arcing. In the airplane, the power-supply box was pressurized at ram pressure with clean hot air bled from the thermal de-icing system. Pressurizing the box prevented any fuel fumes that might have been present in the bomb bay from diffusing into the box.

The trajectories of droplets that entered the ionized field near the luminous region were computed with the use of equation (7) and used to position the cylinders with respect to the cathode. The magnitude of the luminous layer λ was observed in the darkness to be less than 2 millimeters for the conditions of $V_t = 25{,}000$ volts and $l = 7.62$ centimeters. The width of the cylinders was made smaller than the width l by an amount such that, when the cylinders were properly alined with respect to the cathode and the anode, droplets which had at any time been in the luminous region or in the boundary layer of the anode failed to strike the cylinders. The insulators used to mount the cylinders were designed to act also as end plates for the cylinders in order to provide more nearly two-dimensional flow over the cylinders.

The cylinder diameters used were 1/8, 1/2, $1\frac{1}{4}$, and 3 inches. The number of cylinders used of each particular size was governed by the total charge intercepted by each size of cylinder. A larger number of the smaller-sized cylinders was required in order to obtain a measurable current of 2 microamperes. The cylinders of any one size group were wired in parallel. The spacing between cylinders was large enough to avoid aerodynamic interference of the cylinders with each other. Cylinders of the same diameter where ganged together were spaced 14 radii from center to center.

A multiple-recording galvanometer was used to record the variations in current from each set of cylinders. A single-stage amplifier, based on the cathode-follower principle, was used in the circuit between the cylinders and the galvanometer. The current could also be checked in flight with a vacuum-tube microammeter, which was switched into any one circuit when the current reading was desired.

Concern arose as to whether nitrogen or oxygen ions, which may have been present in the coronal-discharge field, could be swept out before they were carried back to the cylinders by the air flow. The mobility constant k for an oxygen molecule is 1.49×10^3. With a

field strength of 10 electrostatic units, the ions move in the x-direction with a velocity of 1.49×10^4 centimeters per second. At an airplane speed of 200 miles per hour, the ions move in the y-direction with a velocity of 8.94×10^3 centimeters per second. An extension of the cathode plate a distance Y_s of 7.5 centimeters (fig. 1) beyond the last source of ions was considered sufficient for the sweep-out field.

FLIGHT RESULTS

The results obtained with the instrument described in the preceding section indicate that the method of charging cloud droplets can be used for some phases of cloud studies. The purpose of the flights described herein was not to obtain conclusive meteorological data but rather to evaluate the method.

The instrument was sensitive in detecting water droplets and other sizable particles present in the atmosphere even on a day apparently clear except for the usual haze noted in the horizon. At an altitude of 4000 feet over Cleveland, a bluish haze was visible between the airplane and the ground. The instrument indicated a sizable current reading on the small cylinders at a true airspeed of 200 miles per hour. The airplane speed was decreased until no current was noted from the small cylinders. The mass of the largest particle which had a trajectory that just failed to reach the 1/8-inch cylinder was calculated with the use of equation (7). If the assumption that the particles are spheres with a density of unity is allowed, the particles had a diameter of 4 microns. A portion of the particle-size spectrum was obtained from the value of the current measured from the 1/8-inch cylinders at a true airspeed of 200 miles per hour and from the trajectories of various-sized particles as calculated with equation (7). The results of this type of analysis indicated that 3×10^5 particles per cubic centimeter, ranging in size from 2 to 4 microns in diameter, were present. No attempt was made to measure particles of smaller size. These results check very well with measurements made by other investigators (reference 9) on condensation nuclei present in the atmosphere on slopes of mountains.

At an altitude of 7000 feet the number of particles was about one-half the number at 4000 feet, but the size range was approximately the same. A region at 7000 feet was found about 30 miles southwest of Cleveland where the instrument indicated nearly clear air. Over Akron, 40 miles southeast of Cleveland, the results were the same as those over Cleveland. Over either city readings of zero current from the cylinders

were not obtained until an altitude of 12,000 feet was attained. A spiraling descent from 12,000 feet over Cleveland indicated that the haze was stratified in two layers, the thinnest part being at approximately 5000 feet. The temperature varied from freezing at 12,000 feet to 10° C at 2000 feet. Several other flights in apparently clear air checked the aforementioned results as to order of magnitude of particle size and content.

On a later flight on a clear and warmer day (temperatures ranged from 23° C near the ground to 17° C at 3500 ft, and 13° C at 7000 ft) immediately after a rain, practically zero readings were obtained from the cylinders at all altitudes. The flight was over Cleveland and at altitudes as high as 7000 feet.

A galvanometer record of the current from three size sets of cylinders registered during a flight through strato-cumulus clouds is presented in figure 8. One inch on the strip corresponds to about 2100 feet in the atmosphere. With records of the type shown, variations occurring in 200 feet of cloud extent can be discerned. The high-frequency variations on the strip are attributed to the natural frequency of the galvanometer elements. In the two top traces, an increase in current is indicated by a downward motion whereas with the 3-inch cylinder record an increase in current reading is up.

Between the lines WW and XX the average liquid-water content, volume-median droplet diameter, and distribution are 0.3 gram per cubic meter, 11 microns, and B, respectively. The large variations recorded to the right of line XX are caused by a cumulus section of the cloud. At the peak conditions the liquid-water content, volume-median droplet diameter, and distribution were 0.9 gram per cubic meter, 8 microns, and C to D or more, respectively. The data were taken at 6000-foot altitude and the average air temperature was about 8° C. The current flow from the set of 1/8-inch cylinders averaged less than 2 microamperes in the stratocumulus clouds and varied up to 5 microamperes in cumulus clouds.

On several occasions stratus clouds were approached from above. On each of these occasions the instrument began indicating liquid-water droplets from 1000 to 500 feet above the apparent cloud. In one 40-mile flight at 8000-foot altitude averaging about 300 feet above a thin stratus cloud, the current measured from the 1/8-inch cylinders fluctuated by as much as 400 percent. Even though the cloud layer was apparently well defined below, columns of moisture rose above the layer.

One flight was made in stratocumulus clouds in the vicinity of the Cleveland Airport and over the south shore of Lake Erie. Observations from the ground before take-off indicated precipitation at the base of some regions of the clouds because of the fuzzy appearance of some spots on the under sides; however, no precipitation reached the ground. Ceiling was reported at slightly over 5000 feet. At 3000-foot altitude, the temperature was 3° C and the current from the different sizes of cylinders was of the same order of magnitude as was noted on previous flights through haze. The air was rough, indicating considerable turbulence. At 6500 feet, the temperature was 0° C and precipitation was encountered in clumps or sheets that varied in length from about 400 to 1500 feet (estimated). On passing through these clumps, the cylinders all read as much as four times the current through other parts of the cloud. A portion of the flight record is shown in figure 9.

Because the instrument was designed without anti-icing equipment, flights were necessarily conducted at atmospheric temperatures above the freezing point. The instrument was flown through slight icing conditions as a matter of curiosity. The only ill effect of the ice noted was a large decrease in current density j, with a consequent loss of signal at both the plugs and the galvanometer. This decrease was attributed to the formation of ice beads on the needle points.

The resistance between the cylinders and the anode was checked during flights through clouds that wetted the instrument to ascertain that the moisture did not cause an appreciable current leakage to the electrical ground. The resistance was always very high, in excess of 700 megohms. Flights were also made under various conditions to determine if atmospheric electricity might be partly the cause of the current measured from the cylinders. With the coronal discharge at zero no current readings were observed from the cylinders. This test indicates that the airplane always assumed the local potentials in the cloud and that the measurements of the instrument were those caused by the additional charge placed on the droplets by the coronal discharge.

CONCLUDING REMARKS

The charged-droplet cloud analyzer is based on a principle that depends in part on the air flow past the instrument. In this respect the instrument fits naturally into the condition encountered when it is used with an airplane. The location of the instrument on the airplane may be improved perhaps to obtain a more representative sample of the clouds. The first model was placed on the bomb-bay doors for convenience in installation.

A difficulty soon realized in the interpretation of the data is the lack of other independent methods for checking the results. The

accuracy in determining the liquid-water content and droplet-size distribution depends on: (1) the error in measuring true airspeed, from which the total charge on each droplet, as well as the rate of cloud interception is obtained; (2) the error in measuring electrical values, particularly the galvanometer readings obtained in the form of traces on films (figs. 8 and 9); and (3) the errors in the assumed distributions presented in table I as compared with the natural conditions found in clouds. With the instrumentation on the airplane used for the tests reported herein, the error in measuring true airspeed is about 2.5 miles per hour, which results in a negligible error in determining liquid-water content and volume-median droplet diameter. For the tests with the instrument described, the errors in measuring and reading electrical values varied depending on the type of cloud encountered, because the errors involved in measuring the current density j and the applied voltage V_t were insignificant as compared with those involved in reading the film records of the galvanometer. Between the lines WW and XX of figure 8, the distribution actually varied from A to C. At any one point a difference of one distribution was possible when read by different observers. At the peak conditions of the cumulus portion of the cloud (fig. 8), the distribution was C or D, depending on the observer. Whether the distribution was C or D changed the liquid-water content by less than 0.1 gram per cubic meter (less than 10 percent of the original). The errors are much larger in resolving the data where the rate of change of cloud conditions is great, such as at the fringes of a cumulus cloud. Under such conditions it is often difficult to distinguish an E distribution from a B distribution. An improvement in the instrumentation and technique of measuring the current from the cylinders will improve the accuracy.

The differences in resolving the data by different observers often lie in that the data obtained from the films do not precisely match any calculated distribution curve. The difficulty in matching the curves is caused in part by the scattering of the data and in part by the difference between the assumed distributions presented in table I and the natural conditions existing in the cloud measured. The addition of cylinders larger than 3 inches in diameter may lessen the uncertainty caused by the scattering of the data.

An instrument based on the method of charging the cloud droplets has the following desirable features:

1. The method can be applied in clouds with temperatures above freezing and perhaps in subfreezing temperatures with proper anti-icing equipment.

2. The size and the shape of the cylinders do not change during the exposure time as in the rotating-multicylinder method.

3. The uncertainty caused by the bouncing off of droplets should be much less than in the rotating-multicylinder method because the transfer of charge from the droplets to the cylinders is nearly instantaneous and what happens to the droplets after the charge is transferred is unimportant.

4. The readings are instantaneous and continuous.

5. The available sensitivity permits the study of the local variations in clouds.

6. Weighing errors are eliminated.

The analysis of clouds is very difficult with any method requiring cylinders or other obstacles to separate the droplets according to their mass, because both the liquid-water content and the droplet sizes in the clouds are unknowns expressed implicitly in the equations employed. An independent method for measuring liquid-water content in the clouds would permit a simplification in the reduction of the data to droplet size distribution.

Lewis Flight Propulsion Laboratory,
National Advisory Committee for Aeronautics,
Cleveland, Ohio, February 16, 1951.

APPENDIX A

SOLUTION OF ELECTRIC-FIELD EQUATIONS

The problem to be solved is the determination of the field strength at points in the field between two parallel plates A and C (fig. 1) with a total applied potential V_t imposed between them. The potential drop is large enough to cause a coronal discharge between the plates. Many attempts to solve the field equations for different ion fields are described in reference 4; but usually simplifications have been necessary to such a degree as to make the results inapplicable to the present problem. In the present report a solution to the field equations is obtained that is complete enough to be of use. The solution is obtained by: (1) the use of the physical conditions that best lend themselves to a solution of the equations, (2) the measurement of as many unknowns as possible, and (3) the use of reasonable simplifying assumptions.

The variation of electrical field strength with position is obtained only in the region between the luminous layer and the anode plate. The assumption is made that in this region the electrons moving toward the anode constitute the only current. This assumption may be somewhat debatable, but it is in agreement, within experimental errors, with probe tests. Calculations employing this assumption are in substantial agreement with experimental observations. These calculations were of the type first made by J. S. Townsend (reference 6) and J. J. Thomson and G. P. Thomson (reference 3) for the case of corona in coaxial cylinders.

In the luminous layer, the current is the sum of that due to the electrons moving toward the anode and that due to the positive ions moving toward the cathode. Although an exact solution would be desirable, it has not been found necessary for solution of the problem for the charged droplets. An observation in darkness of the magnitude of λ is all that is necessary. A knowledge of the magnitude of λ is necessary in order to position the cylinders properly.

If the field in the nonluminous region is assumed independent of the y- and z-directions, Poisson's equation for the electric field becomes

$$\frac{d^2V}{dx^2} = -4\pi\rho \tag{A1}$$

The assumption that $\partial V/\partial y$ and $\partial V/\partial z$ are zero is not strictly correct near the needle points; however, the cathode plate aids in obtaining a uniform field over most of the distance from λ to the anode. The

assumption is made that the charge density ρ is composed only of negatively charged electrons. This last assumption also implies that the current density is constant in the region considered.

Poisson's equation will first be used to solve for the field intensity E_0, which is here defined as the force at a point in the electric field that would be exerted on a unit positive charge. From the usual definition of the potential, the expression is obtained:

$$E_0 = -\frac{dV}{dx} \tag{A2}$$

The current density at any point x is

$$j = \rho v'_x = \rho k E_0 = -\rho k \frac{dV}{dx} \tag{A3}$$

where

j flow of positive electricity per unit cross-sectional area in unit time

v'_x drift velocity of electrons

Experiments have demonstrated the mobility k to be nearly a constant, over a considerable range of field strength, for a particular ion in a given atmosphere (reference 4).

The use of equation (A3) in Poisson's equation (A1) yields

$$\frac{dV}{dx}\frac{d^2V}{dx^2} = \frac{4\pi j}{k} \tag{A4}$$

from which by integration and substitution of equation (A2)

$$\left(\frac{dV}{dx}\right)^2 = E_0^2 = \frac{8\pi j x}{k} + C_1^2 \tag{A5}$$

and

$$V = \pm\frac{k}{12\pi j}\left(\frac{8\pi j x}{k} + C_1^2\right)^{\frac{3}{2}} + C_2 \tag{A6}$$

where C_1 and C_2 are constants of integration. The constants of integration are evaluated by applying the boundary conditions that the anode is grounded and that the cathode is charged to a potential $-V_t$. A question arises as to the validity of applying the boundary condition that $V = -V_t$ when $x = l$, because this condition implies that equation (A5) also applies in the luminous region. The justification is in the experimental evidence (references 7, 10, and 11, and unpublished work at the Lewis laboratory). For large values of dV/dx, in the order of 2500 volts per centimeter or more, the rate of change of potential with respect to distance is nearly the same in the luminous region as in the nonluminous region. The references cited present results with coaxial cylindrical electrodes, but there is no reason for expecting that ionization principles are different for the plane parallel electrodes in the problem presented herein. The error in the determination of E_0 from applying the aforementioned boundary conditions is negligible with high voltage drops and low values of j, as is true in the instrument for which these equations are derived.

The current density j is measured with a microammeter that is connected between the ground and a known area of the anode (figs. 1 and 6). Several of these elements of anode area are located where plate and effects are least, and are insulated from the remainder of the anode, which is directly connected to ground. The mobility k is obtained from Langevin's equation (reference 4)

$$k = 0.75 \frac{\epsilon}{m_\epsilon} \frac{\lambda'}{\bar{c}_1} \tag{A7}$$

where

ϵ/m_ϵ ratio of charge to mass of electron

λ' mean free path of electrons

$\bar{c}_1$ average random velocity of electrons determined from Maxwell-Boltzmann velocity-distribution curve

The mean free path of electrons is obtained from

$$\lambda' = 4\sqrt{2}\, L = 5.6\, L$$

where L is mean free path of air molecules (reference 4) and

$$\bar{c}_1 = 0.922 \sqrt{\frac{3k'T}{m_\epsilon}}$$

where

k' Boltzmann constant

T absolute temperature

Compton's more accurate equation (reference 4) for the electron mobility is not used because the refinement gained thereby is unwarranted for the present purpose.

From the application of the first boundary condition that $V = 0$ for $x = 0$ in equation (A6)

$$C_2 = - \frac{k}{12\pi j} C_1^3 \tag{A8}$$

and from the second boundary condition that $V = - V_t$ for $x = l$

$$- V_t = \frac{\pm k}{12\pi j} \left[\left(\frac{8\pi j l}{k} + C_1^2 \right)^{\frac{3}{2}} - C_1^3 \right] \tag{A9}$$

The constant C_1 may be explicitly evaluated by expanding the term raised to the 3/2 power by the binomial theorem and retaining the first two terms of the expansion. This operation is permissible when $8\pi jl/k$ is small compared with C_1. The constant is

$$C_1 = \pm \frac{V_t}{l} \tag{A10}$$

The substitution of this value for C_1 into equation (A5) results in

$$E_0^2 = \frac{8\pi j x}{k} + \left(\frac{V_t}{l} \right)^2 \tag{1}$$

which is the required field intensity.

The effect of space charge on E_0 was very small in the experimental model described in the section titled "Description of Instrument." The highest value of current density recorded was $j = \frac{1}{3} \times 10^{-6}$ ampere $= 1 \times 10^3$ electrostatic units; $V_t = 25{,}000$ volts $= 83.3$ electrostatic units; $l = 7.62$ centimeters; $k = 2.02 \times 10^6$ electrostatic units. For these values, equation (1) becomes

$$E_0^2 = \frac{(8\pi)(1 \times 10^3)x}{2.02 \times 10^6} + \left(\frac{83.3}{7.62}\right)^2$$

from which it is seen that the term containing x is very small compared with the other term on the right because $0<x<l$, and equation (1) may be written

$$E_0 = \frac{V_t}{l} \tag{2}$$

For the instrument used in the tests, no serious error was made in the final results by ignoring the effect of the current density on E_0; however, this would not be true for instruments in which j is an appreciable quantity.

APPENDIX B

RATE OF CHARGE ACQUISITION BY WATER DROPLET IN IONIZED FIELD

The rate of acquisition of charge is derived for a droplet located in an ionized field. The spherical droplet acquires charge by electrical attraction of the electrons. The electrons follow the lines of force that lead to the droplet (fig. 2). In this manner, the droplet ceases to acquire more electrons from the field when the radial force of attraction between the electrons in the field and the droplet is zero or negative for all angles of approach. For reasons of simplicity, the theory is developed for spherical droplets that are perfect conductors and then discussed for droplets, such as water droplets, that have a specific inductive capacitance of σ.

A conducting droplet (fig. 3) of radius a with center O and with a charge Q is considered located at a coordinate point x, where the field E_0 is determinable from equation (1) or (2). The objective is to derive the expression for the radial component of the force exerted on an electron of charge ϵ situated at a neighboring point P a distance r from O. The derivation is based on the assumptions listed previously in the section entitled "Principle of Operation."

Derivation of Equations

The radial component of the force of attraction between the droplet and the electron is given by equation (3). For ease in evaluating the significance of the equation, a transformation is made in the form of $r = a(1+\nu)$. In this manner the distance from the surface of the droplet to the electron is given as a fractional part of the radius, that is, by ν.

$$F_r = -\left\{\left[1 + \frac{2}{(1+\nu)^3}\right]\epsilon E_0 \cos\theta\right\} - \left[\frac{\epsilon Q}{a^2(1+\nu)^2}\right] - \left\{-\frac{\epsilon^2(1+\nu)}{a^2 4\nu^2\left[1+\nu+\left(\frac{\nu}{2}\right)^2\right]} + \frac{\epsilon^2}{a^2(1+\nu)^3}\right\} \tag{B1}$$

The charges represented by ϵ and Q are negative, and therefore electrons will no longer be forced on to the droplet when it has acquired sufficient charge Q to make F_r zero or negative anywhere in the field for all polar angles θ of electron approach. When the value of ν is large compared to ϵ, the last braced term of equation (B1), the image term, contributes very little to the value for F_r. If a space surrounding the droplet is considered in which the image terms are negligible, it becomes evident that F_r is negative for all values of θ between $\pi/2$ and $3\pi/2$ regardless of the amount of charge. As the charge Q acquired by the droplet increases in magnitude, the force F_r becomes zero for successively smaller values of the polar angle θ. Thus, the charge can be imagined funneled through a cone for which the half-vertex angle θ decreases as the amount of charge Q acquired by the droplet increases (fig. 2).

The variation of F_r experienced by electrons approaching the droplet along the x-axis, where $\theta = 0$, for three values of Q is shown in figure 10. The last term in equation (B1), which represents the mutual force of attraction between the electrons and the droplet, contributes greatly to the magnitude of F_r only for small values of ν, that is, when the electron is very near the surface. An electron approaching the negatively charged droplet is acted on by a diminishing force of attraction, which may become zero or repulsive for sufficiently high charge on the droplet, until the mutual force of attraction becomes large enough to cause the attractive force to increase again. The droplet is considered fully charged when it has been charging long enough to have raised the magnitude of Q to that required to make F_r zero anywhere along the zero polar axis. Additional electrons will be attracted to the sphere only if they have sufficient kinetic energy from thermal agitation or previous motion to carry them through the region where F_r is zero. The charge thus acquired does not, in principle, have any definite limit; however, the number of electrons that have a high velocity is small and the droplet is in the region of ionization for only a short time. This type of charging is of minor consequence in the instrument under consideration.

The image term may be neglected without appreciable error in the expression for the force of attraction provided that the results apply to conditions in which $(a\nu)^2$ is much greater in magnitude than ϵ^2. The value of ϵ is 4.803×10^{-10} electrostatic unit (reference 12). For droplets with a radius of 10 microns (10^{-3} cm) the error resulting from neglecting the image term is small for regions where ν is greater than 10^{-4}. Because of the mutual attraction between the electron and the droplet, the escape of electrons from the surface of the sphere is very improbable. When the image term is ignored, the expression for the electric potential at the position of the electron becomes

$$V = - \left(1 - \frac{a^3}{r^3}\right) E_0 r \cos \theta + \frac{Q}{r} \tag{B2}$$

The rate of accumulation of charge by a droplet is best determined from a consideration of the function for the lines of force surrounding a sphere located in an electric field. From Lamb (reference 13, pp. 127 and 128), the function is obtained for the lines of force, which are orthogonal to the equipotential lines given by equation (B2). Lamb gives the force-field functions in terms of the zonal harmonics P_n as

$$\psi_1 = \frac{1}{n+1} r^{n+1} (1-\mu^2) \frac{dP_n}{d\mu}$$

$$\psi_2 = - \frac{1}{n} r^{-n} (1-\mu^2) \frac{dP_n}{d\mu}$$

and

$$\psi_3 = - (1 - \mu)$$

where n is the order of the zonal harmonic and μ is assigned the value of $\cos \theta$ for a problem involving a sphere.

The zonal harmonics (reference 13, p. 115) that suit the problem under consideration result in the following force-field function:

$$\psi = \psi_1 + \psi_2 + \psi_3 = \left(A \frac{r^2}{2} + \frac{B}{r}\right) \sin^2 \theta + C(1 - \cos \theta) \tag{B3}$$

where A, B, and C are arbitrary constants to be evaluated by the boundary conditions. The x-component of the local field strength is obtained from the force-field function by the expression

$$E_x = - \frac{1}{\omega} \frac{\partial \psi}{\partial \omega} \tag{B4}$$

where ω is defined by the relation

$$r^2 = x^2 + y^2 + z^2 = x^2 + \omega^2 \tag{B5}$$

(figs. 2 and 3). The relations

$$\cos \theta = \frac{x}{r} \tag{B6}$$

and

$$\sin \theta = \frac{\omega}{r} \tag{B6a}$$

are obtained from the geometry and equation (B5).

The first boundary condition to be applied is that

$$E_x = E_0 \tag{B7}$$

when r is very large compared to the droplet radius a. The substitution of equations (B6) and (B6a) into equation (B3) yields

$$\frac{\partial \psi}{\partial \omega} = A\omega + \frac{2B\omega}{r^3} - \frac{3B\omega^3}{r^5} + \frac{Cx\omega}{r^3} \tag{B8}$$

because $\partial r^2/\partial \omega = 2\omega$ from equation (B5). As r approaches ∞, equation (B8) reduces to

$$\frac{\partial \psi}{\partial \omega} = A\omega \tag{B9}$$

The combination of equations (B4), (B7), and (B9) yields

$$A = -E_0$$

The other boundary condition is applied very near the surface of the sphere where $r \approx a$, $x \approx a$, and $\theta = 0$. Differentiation in equation (B4) gives

$$E_x = E_0 - \frac{2B}{a^3} - \frac{C}{a^2} \tag{B10}$$

From the definition of the field strength

$$E_x = (E_r)_{\substack{\theta=0, \\ r=x=a}} = 3E_0 + \frac{Q}{a^2} \tag{B11}$$

because from equation (B2)

$$E_r = \left(1 + \frac{2a^3}{r^3}\right) E_0 \cos \theta + \frac{Q}{r^2}$$

The first term on the right in equation (B11) gives the effect of the external field E_0, as modified by the presence of the spherical droplet, and the second term the effect of the accumulated charge Q. A comparison of equations (B10) and (B11) yields

$$B = -E_0 a^3 \quad \text{and} \quad C = -Q$$

The final form of ψ is

$$\psi = -E_0 \left(\frac{r^2}{2} + \frac{a^3}{r}\right) \sin^2 \theta - Q(1 - \cos \theta) \tag{B12}$$

This expression is the equation for the lines of force along which the electrons flow.

At some point in the field near the surface of the droplet, where $r = a(1+\nu)$ and ν is large enough to make the image terms of equation (B1) negligible but small enough numerically that $r \approx a$, some value of θ exists for a given value of Q for which F_r is zero. Here the lines of force are normal to the radius; and there are no lines of force, which originated at some distance from the droplet, terminating on the droplet for θ greater than this particular value. This angle is denoted by θ_0, and from equation (B1)

$$\cos \theta_0 = -\frac{Q}{3E_0 a^2} \tag{B13}$$

The equation of the line of force passing through the point where $r \approx a$ and $\theta = \theta_0$ is

$$\frac{3}{2} E_0 a^2 \left[1 - \frac{Q^2}{(3E_0 a^2)^2}\right] + Q\left(1 + \frac{Q}{3E_0 a^2}\right) = E_0 \left(\frac{\omega^2}{2} + \frac{a^3 \omega^2}{r^3}\right) + Q\left(1 - \frac{x}{r}\right)$$

from equation (B6), (B6a), and (B12). For very large values of r and x

$$\omega^2 = 3a^2 \left[1 - \frac{Q^2}{(3E_0 a^2)^2}\right] + \frac{2Q}{E_0}\left(1 + \frac{Q}{3E_0 a^2}\right) = \frac{1}{3E_0{}^2 a^2}(3E_0 a^2 + Q)^2 \tag{B14}$$

Physically, ω in this equation is the radius at a large distance from the droplet of the largest force tube for which all the enclosed lines of force terminate on the droplet. All lines of force outside this force tube do not intercept the droplet. Electrons that were initially enclosed by this force tube will impinge on the droplet.

The rate of negative charge acquisition is determined with the aid of equation (B14) and by solving for

$$\frac{dQ}{dt} = j\pi\omega^2 = \frac{j\pi}{3E_0{}^2a^2}\left(3E_0a^2 - Q\right)^2$$

$$\frac{dQ}{\left(3E_0a^2 - Q\right)^2} = \frac{j\pi}{3E_0{}^2a^2}\,dt$$

$$Q = \frac{3\pi a^2E_0jt}{E_0 + j\pi t} \tag{B15}$$

For large values of time t

$$Q_\infty = 3E_0a^2 \tag{5}$$

The value for E_0 is obtained from equation (1). As was previously stated, the current density j in the instrument built was small enough that E_0 was virtually constant in the nonluminous region. For this instrument, the droplets acquired the same charge regardless of the x-position through which they passed in the nonluminous region. If j is appreciable, the charge acquired depends on the value of x. In order that relation (B15) apply, j must be sufficiently small that the first assumption of uniform field in the neighborhood of the sphere is valid.

The effect of the specific inductive capacitance σ of the water droplet on the charge acquired can be determined by rewriting the potential expression (equation (B2)) as

$$V = -\left(1 - \frac{\sigma-1}{\sigma+2}\frac{a^3}{r^3}\right)E_0r\cos\theta + \frac{Q}{r}$$

If the required changes were made in the process of development, the final result would be

$$Q = \left(1 + 2\,\frac{\sigma-1}{\sigma+2}\right)\frac{\pi a^2E_0jt}{E_0 + j\pi t} \tag{4}$$

and

$$Q_\infty = \left(1 + 2\,\frac{\sigma-1}{\sigma+2}\right)E_0a^2$$

Inasmuch as $\sigma = 81$ for water, the effect of the specific inductive capacitance is practically negligible.

Experimental Verifications

An attempt was made to check experimentally the amount of charge acquired by metallic spheres in falling through a region of coronal discharge. The spheres were individually dropped through an ionized atmosphere that existed between cathode and anode plates, similar to the setup illustrated in figure 1. The spheres were caught below the ionized region in a small metallic cup electrically connected to a quadrant electrometer. With this arrangement, only spheres of 250-micron radius or larger acquired sufficient charge to allow accurate measurements with the electrometer. The smallest sphere used was perhaps 20 times larger in diameter than the estimated average droplet size in clouds.

The most consistent results were obtained when the spheres remained in the charging field long enough to acquire nearly the saturation charge, expressed by equation (5). Under these conditions the measured charge averaged approximately 2 percent less than the value calculated with the use of equation (B15). The time the spheres remained in the charging field was varied by changing the average velocity of the sphere through the field. The velocity was changed by varying the starting height above the field. If the height from which large spheres were dropped was so chosen that the acquired charge was equal to the charge acquired by smaller spheres dropped from lower heights, the discrepancy between the measured and calculated value of Q was still about 2 percent.

The quadrant-electrometer method used in the experiments described was insufficiently accurate to verify experimentally equation (B15) when particles as small as cloud droplets were of interest. A method employing the principle of the mass spectrometer to separate particles according to the ratio of charge to mass may, perhaps, fulfill the need. In this spectrometer method, the charge acquired by a sphere might be measured by noting the effect of a known electrostatic field on a moving charged sphere of known mass.

APPENDIX C

TRANSLATION OF CURRENT MEASUREMENTS INTO DROPLET-SIZE DISTRIBUTION

The procedure for determining the electrical collection efficiency E_c for the A distribution of table I is explained in the section entitled "Principle of Operation." For the other distributions of table I, the procedure is explained with the use of a sample calculation for the B distribution. The electrical collection efficiency E_c for the B distribution is essentially a modification of the mass collection efficiency calculated with the differential analyzer (reference 1) for the A distribution. The over-all E_c of the B distribution is found from the sum of the contributions of each size group in the B distribution.

In the work of reference 1 on the impingement of cloud droplets on cylinders moving through the cloud, three convenient dimensionless parameters were used:

$$\left.\begin{aligned} \Phi &\equiv \frac{18\rho_a{}^2 LU}{\mu\rho_w} \\ K &\equiv \frac{2}{9}\frac{\rho_w a^2 U}{\mu L} \end{aligned}\right\} \qquad \text{(C1)}$$

and

$$K\Phi \equiv \left(\frac{2\rho_a a\ U}{\mu}\right)^2$$

The collection efficiency is expressible in terms of the dimensionless quantities $K\Phi$ and K, which are listed in table III. The values of $K\Phi$ were chosen to cover a wide range of air speeds and droplet sizes. The example chosen for presentation herein is worked for a $K\Phi$ value of 200.

As a basis for beginning the computations, a value of $1/K = 4.0$ is assigned to those droplets in the volume-median group size. (This particular value for $1/K$ was chosen to correspond to one of the values of $1/K$ arbitrarily chosen in reference 1 for the computations for E_M.) The effect of the variation of the group size on $1/K$ is obtained by dividing the assumed value of $1/K$ $(1/K = 4.0)$ by $(a/a_0)^2$, because the radius appears to the second power in equation (C1). The results are shown in the fourth column of table IV. The collection efficiency E_c for each value of $1/K$ thus computed is obtained by interpolation

of table III. The values of E_c corresponding to $K\Phi = 200$ are shown in the fifth column of table IV.

The next step is to determine what contribution each size group makes to the total E_c for the B distribution. A term τ must be defined as the ratio of the electrical charge contained in the particular group in question compared with the total of the charge contained in all the groups. For example,

$$\tau_1 = \frac{N_1 a_1^2 \left(\frac{3\pi E_0 jt}{\pi jt + E_0}\right)}{\left(\frac{3\pi E_0 jt}{\pi jt + E_0}\right)\left(N_1 a_1^2 + N_2 a_2^2 + \ldots N_7 a_7^2\right)}$$

$$\tau_2 = \frac{N_2 a_2^2}{N_1 a_1^2 + N_2 a_2^2 + \ldots N_7 a_7^2}$$

$$\ldots$$

$$\tau_7 = \frac{N_7 a_7^2}{N_1 a_1^2 + N_2 a_2^2 + \ldots N_7 a_7^2}$$

where N is the number of drops in each size group and the subscripts refer to the group number in table IV. The values for N are determined from seven relations involving the percentage mass in each group size:

$$0.05 = \frac{N_1 a_1^3}{N_1 a_1^3 + N_2 a_2^3 + \ldots N_7 a_7^3}$$

$$\ldots$$

$$0.30 = \frac{N_4 a_4^3}{N_1 a_1^3 + \ldots N_7 a_7^3}$$

$$\ldots$$

$$0.05 = \frac{N_7 a_7^3}{N_1 a_1^3 + \ldots N_7 a_7^3}$$

The values of τ are presented in the sixth column of table IV.

The E_c for the B distribution when $K\Phi = 200$ is the sum of the individual contributions of each size group:

$$E_c = E_{c,1}\tau_1 + \cdots + E_{c,7}\tau_7$$

The value of E_c thus obtained is presented as the last figure in the seventh column of table IV and is listed in table II. The process is repeated for all the other values of $1/K$ and $K\Phi$ given in table II.

The data necessary from flight are the true airspeed U, the air viscosity μ, the air density ρ_a, and the current per unit projected area from each different size of cylinders. On log-log paper the current per unit of projected cylinder area is plotted as the abscissa and the cylinder diameter as the ordinate (fig. 11). A standard value of $K\Phi$ that corresponds most closely to the flight conditions is chosen from table II. As only an approximate value of $K\Phi$ is needed to give a fairly accurate result, it is permissible to estimate the volume-median drop size so that a first-approximation value of $K\Phi$ can be calculated to aid in the choice of the standard value of $K\Phi$. The five columns corresponding to five distributions of droplet sizes for the standard value of $K\Phi$ chosen are plotted on log-log paper, E_c as the abscissa and $1/K$ as the ordinate (fig. 12). Log-log paper should be used because multiplication of the value on one axis corresponds merely to a displacement along that axis. Because E_c and current per unit of projected cylinder area are proportional and because $1/K$ is proportional to the cylinder diameter 2L, the plotted points of figure 11 closely coincide with one of the curves of figure 12 when the two sheets of paper are superimposed and shifted horizontally and vertically (not rotated), provided $K\Phi$ was estimated fairly closely. The best fit of the experimental curve of figure 11 with one of the computed curves of figure 12 is shown in figure 12.

If the estimated value for $K\Phi$ is incorrect, the curve of figure 11 cannot be made to coincide with any of the curves of figure 12. If the curves do not coincide, figure 11 is matched with plots of $1/K$ against E_c for other values of $K\Phi$. A method for interpolating $K\Phi$ is presented in references 1 and 8.

REFERENCES

1. Langmuir, Irving, and Blodgett, Katherine B.: A Mathematical Investigation of Water Droplet Trajectories. Tech. Rep. No. 5418, Air Materiel Command, AAF, Feb. 19, 1946. (Contract No. W-33-038-ac-9151 with Gen. Elec. Co.)

2. Katz, R. E., and Cunningham, R. M.: Aircraft Icing Instruments. Instruments for Measuring Atmospheric Factors Related to Ice Formation on Airplanes - II. Dept. Meteorology, M.I.T., March 1948. (Final Rep. under Air Force Contract No. W-33-038-ac-14165, July 1, 1945-Dec. 31, 1947.)

3. Thomson, J. J., and Thomson, G. P.: Conduction of Electricity through Gases. Vols. I and II. Cambridge Univ. Press, 3d ed., 1928.

4. Loeb, Leonard B.: Fundamental Processes of Electrical Discharge in Gases. John Wiley & Sons, Inc., 1939.

5. Cobine, James Dillon: Gaseous Conductors. McGraw-Hill Book Co., Inc., 1941.

6. Townsend, J. S.: Electricity in Gases. Clarendon Press (Oxford), 1915, p. 378.

7. Pauthenier, et Mallard: Contribution à l' étude du champ cylindrique dans l' air ionisé à la pression ordinaire. Contrôle expérimental. Comptes Rendus, T. 189, Nr. 21, Nov. 18, 1929, P. 843-845.

8. Anon.: The Multicylinder Method. The Mount Washington Observatory Monthly Res. Bull., vol. II, no. 6, June 1946.

9. Anon.: Handbook of Meteorology, F. A. Berry, E. Bollay, and Norman R. Beers, eds. McGraw-Hill Book Co., Inc., 1945.

10. Ladenburg, Rudolf: Untersuchungen über die physikalischen Vorgänge bei der sogenannten elektrischen Gasreinigung. Teil I. Über die maximale Aufladung von Schwebeteilchen. Ann. d. Phys., Bd. 4, Heft 7, Folge 5, 1930, S. 863-897.

11. Deutsch, Walther: Bewegung und Ladung der Elektrizitätsträger im Zylinderkondensator. Ann. d. Phys., Bd. 68, No. 12, Folge 4, 1922, S. 335-344.

12. Richtmeyer, F. K., and Kennard, E. H.: Introduction to Modern Physics. McGraw-Hill Book Co., Inc., 4th ed., 1947.

13. Lamb, Horace: Hydrodynamics. Dover Pub., 6th ed., 1945.

TABLE I - FIVE ASSUMED DISTRIBUTIONS OF DROPLET SIZE

[Size is expressed as ratio of average drop radius in each group to volume-median drop radius a_0. Table is taken from reference 1.]

Total liquid water in each group size (percent)	Distributions				
	A	B	C	D	E
5	1.00	0.56	0.42	0.31	0.23
10	1.00	.72	.61	.52	.44
20	1.00	.84	.77	.71	.65
30	1.00	1.00	1.00	1.00	1.00
20	1.00	1.17	1.26	1.37	1.48
10	1.00	1.32	1.51	1.74	2.00
5	1.00	1.49	1.81	2.22	2.71

Example of interpretation: 30 percent of the liquid-water content of any cloud is contained in droplets that have a radius a_0. In the case of the B distribution, 20 percent of the liquid-water content is contained in droplets that have a radius smaller than the volume-median radius a_0 by a ratio $a/a_0 = 0.84$ and another 20 percent in droplets that have a radius larger than a_0 by a ratio $a/a_0 = 1.17$. A similar interpretation applies to the remaining values.

TABLE II - VALUES OF ELECTRICAL COLLECTION EFFICIENCY E_c

FOR DROPLET-SIZE DISTRIBUTIONS A, B, C, D, AND E

1/K	E_c									
	$K\Phi = 0$					$K\Phi = 20$				
	A	B	C	D	E	A	B	C	D	E
4.0	0.040	0.049	0.053	0.055	0.067	0.030	0.037	0.040	0.043	0.054
2.0	.187	.171	.158	.143	.146	.137	.129	.125	.117	.123
1.0	.385	.343	.306	.271	.246	.326	.289	.261	.233	.215
.5	.560	.521	.476	.419	.400	.522	.477	.431	.380	.363
.2	.761	.723	.681	.619	.581	.729	.692	.646	.584	.548
.1	.864	.836	.800	.746	.704	.843	.812	.776	.717	.675
.05	.927	.912	.884	.842	.790	.916	.897	.867	.824	.765
.02	.970	.961	.948	.925	.895	.963	.954	.939	.913	.882
.01	.984	.981	.974	.959	.943	.983	.978	.970	.953	.934
	$K\Phi = 200$					$K\Phi = 1000$				
4.0	0.021	0.027	0.030	0.033	0.044	0.015	0.020	0.022	0.026	0.035
2.0	.101	.100	.099	.095	.104	.076	.077	.078	.077	.086
1.0	.271	.246	.224	.201	.186	.226	.203	.187	.170	.159
.5	.478	.432	.390	.342	.330	.420	.379	.342	.303	.294
.2	.694	.656	.609	.548	.515	.656	.613	.567	.506	.478
.1	.822	.788	.748	.687	.646	.796	.756	.715	.652	.612
.05	.904	.883	.851	.802	.739	.886	.861	.826	.773	.709
.02	.961	.949	.932	.902	.871	.951	.938	.918	.886	.853
.01	.983	.977	.966	.947	.926	.980	.968	.957	.935	.913
	$K\Phi = 3000$					$K\Phi = 10,000$				
4.0	0.011	0.015	0.018	0.021	0.029	0.009	0.011	0.013	0.016	0.022
2.0	.060	.062	.064	.064	.073	.044	.048	.051	.051	.059
1.0	.186	.172	.167	.148	.139	.149	.139	.131	.123	.116
.5	.373	.339	.306	.272	.265	.314	.288	.263	.236	.234
.2	.624	.579	.531	.475	.449	.582	.533	.487	.433	.411
.1	.767	.729	.686	.622	.585	.736	.695	.649	.585	.551
.05	.870	.843	.806	.750	.685	.848	.820	.779	.719	.654
.02	.943	.928	.907	.872	.837	.932	.915	.891	.852	.813
.01	.971	.963	.950	.926	.902	.965	.955	.941	.914	.887

TABLE III - VALUES OF E_M AND E_c FOR DISTRIBUTION A AS FUNCTION OF $1/K$ FOR VARIOUS VALUES OF $K\Phi$

[Table from reference 1.]

$1/K$	$E_M = E_c$					
	$K\Phi$					
	0	20	200	1000	3000	10,000
4.0	0.040	0.030	0.021	0.015	0.011	0.009
2.0	.187	.137	.101	.076	.060	.044
1.0	.385	.326	.271	.226	.186	.149
.5	.560	.522	.478	.420	.373	.314
.2	.761	.729	.694	.656	.624	.582
.1	.864	.843	.822	.796	.767	.736
.05	.927	.916	.904	.886	.870	.848
.02	.970	.963	.961	.951	.943	.932
.01	.984	.983	.983	.985	.971	.965

TABLE IV - SAMPLE CALCULATIONS FOR E_c FOR DISTRIBUTION B, AND $K\Phi = 200$

[$1/K$ for volume-median drop size assigned value 4.0.]

Group number	$\frac{a}{a_0}$	Percentage in each size group	$\frac{1}{K}$	E_c	τ	τE_c
1	0.56	5	12.73	0	0.085	0
2	.72	10	7.72	.003	.133	.0004
3	.84	20	5.68	.008	.227	.0018
4	1.00	30	4.00	.023	.287	.0066
5	1.17	20	2.92	.050	.163	.0082
6	1.32	10	2.29	.081	.072	.0058
7	1.49	5	1.82	.118	.032	.0038
						$\Sigma = 0.0266$

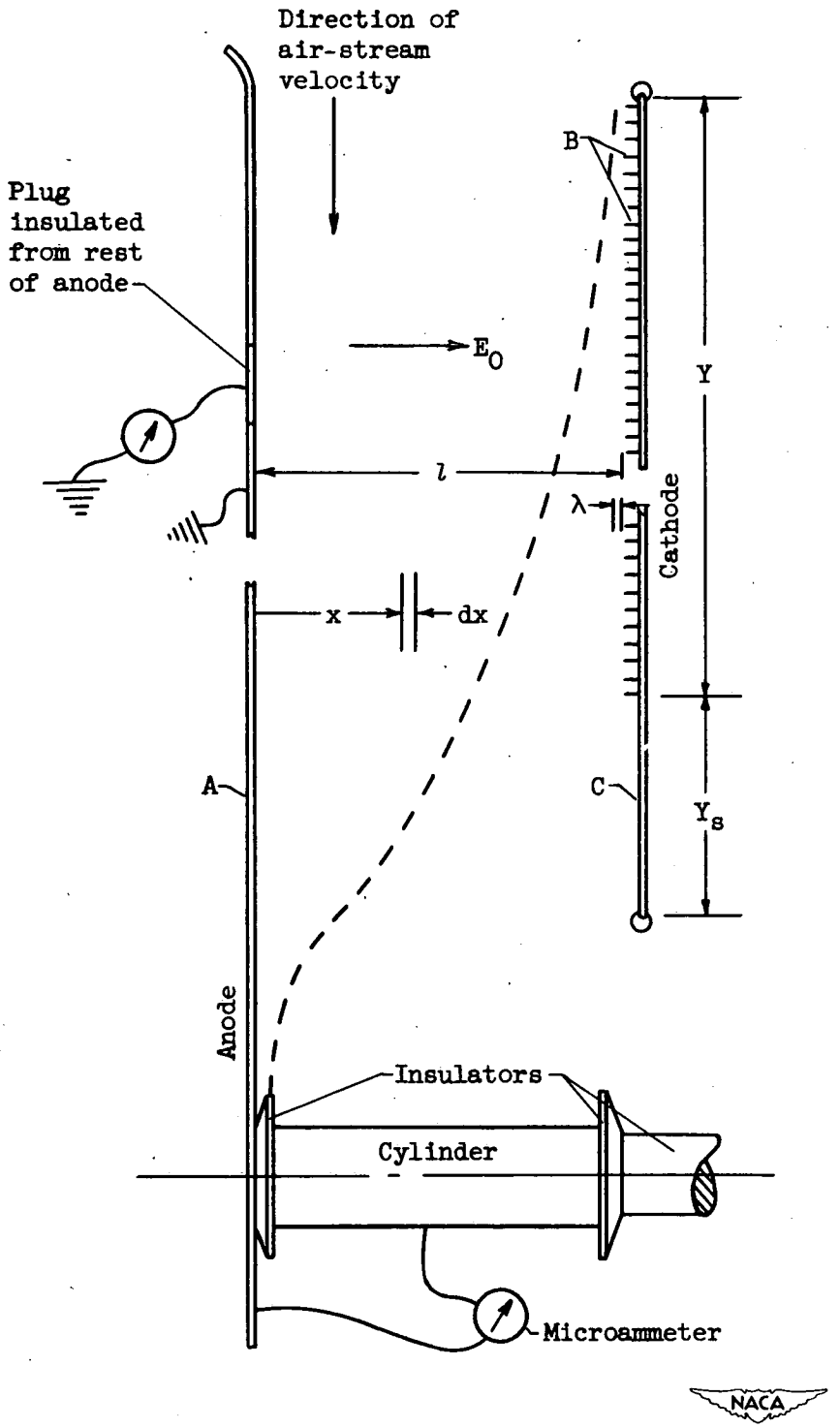

Figure 1. - Schematic drawing of coronal-discharge field.

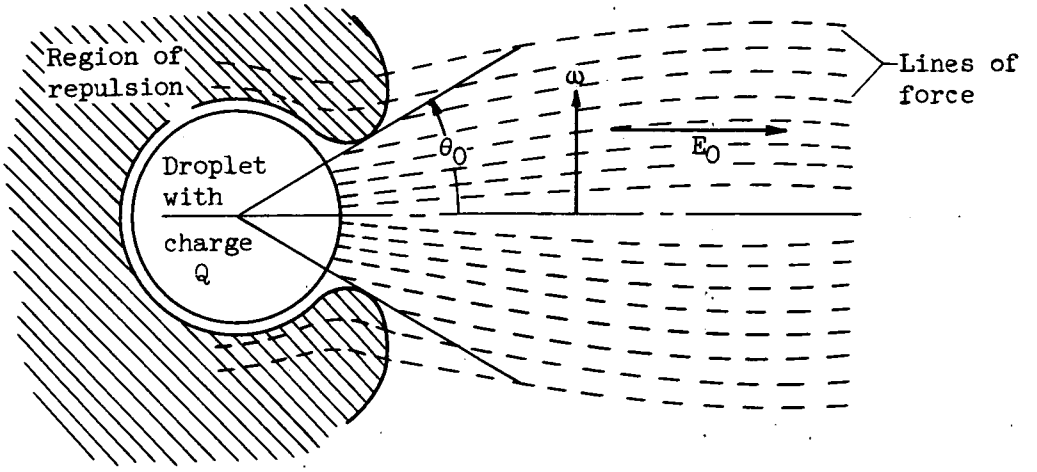

Figure 2. - Diagram of force field around charged droplet.

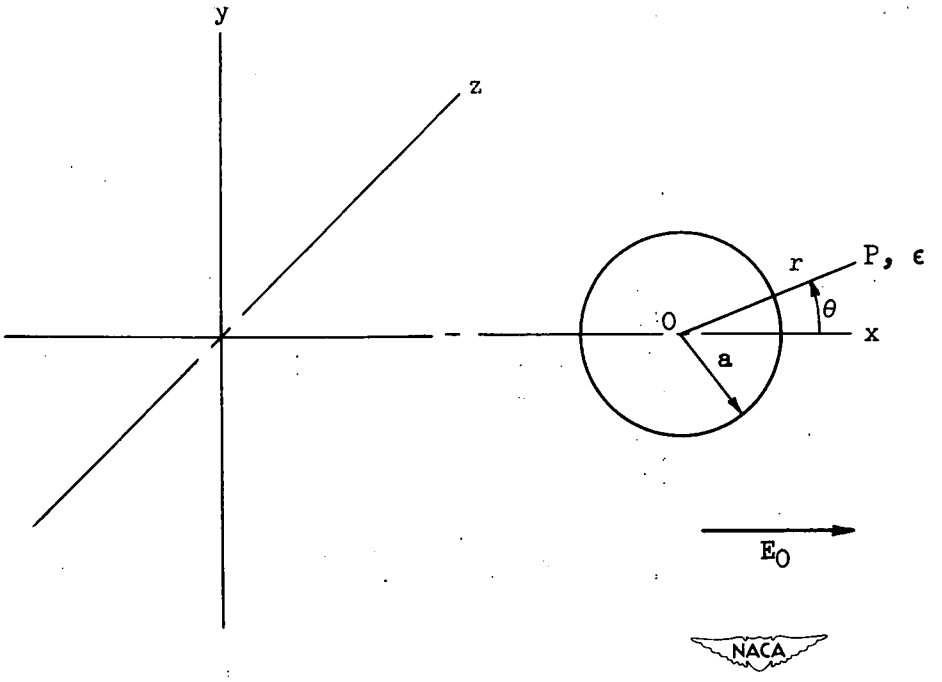

Figure 3. - Diagram of droplet in electric field.

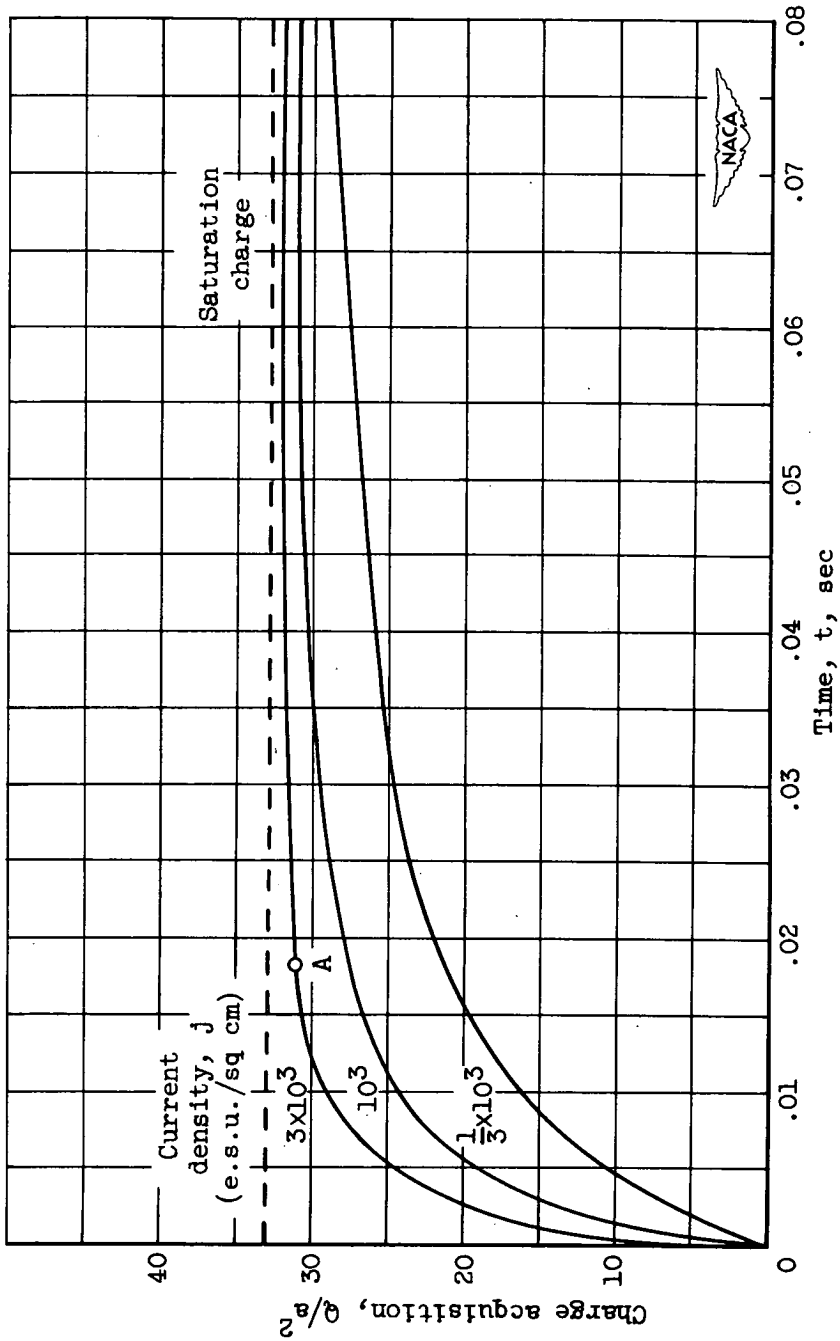

Figure 4. - Charge acquisition by droplet with respect to time in electric field. Undisturbed electric field strength E_0 = 10.92 electrostatic units per centimeter.

Page intentionally left blank

Page intentionally left blank

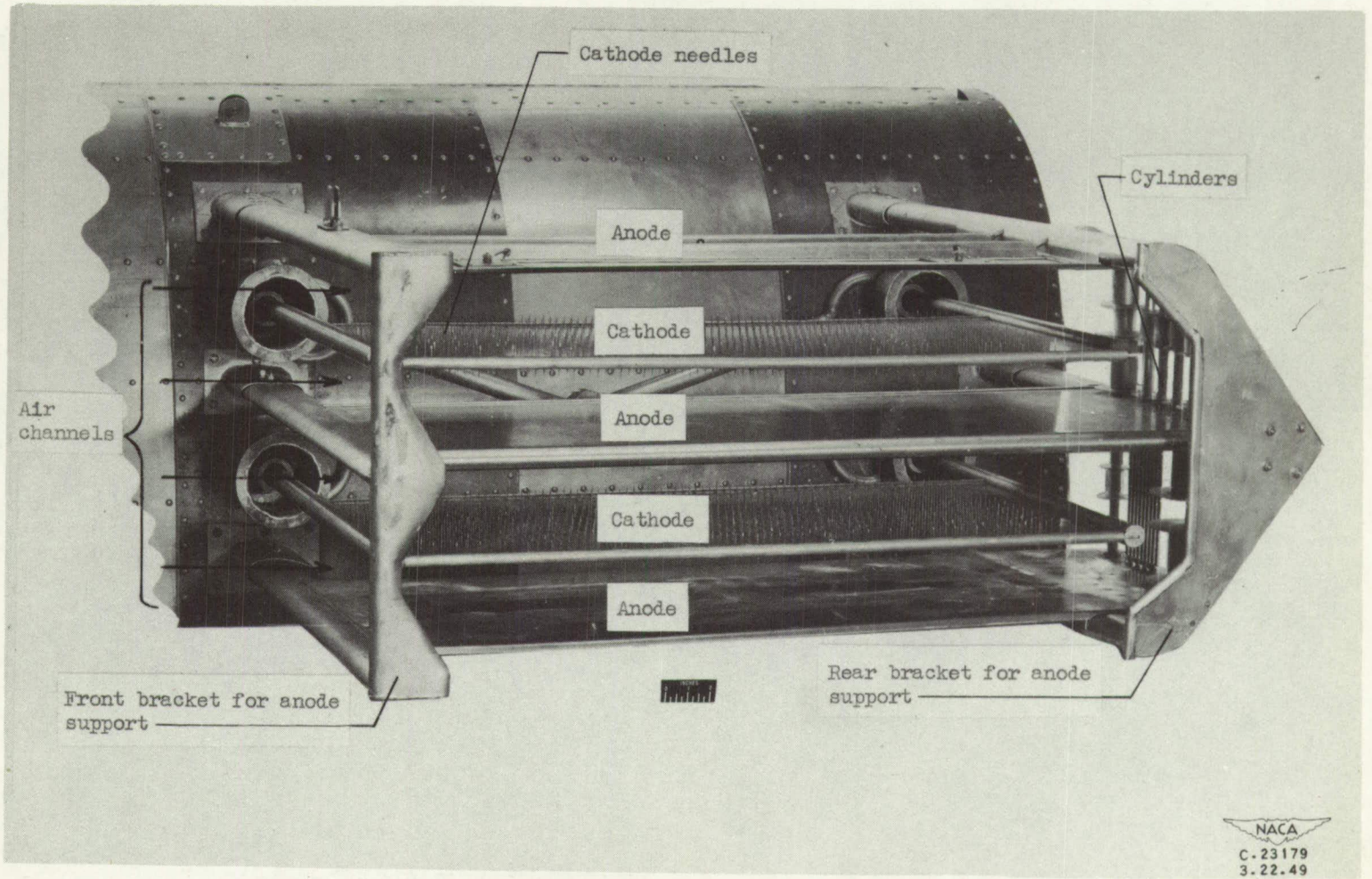

Figure 5. - Bottom view of charged-droplet cloud analyzer. Arrows indicate direction of air stream through the channels.

Page intentionally left blank

Page intentionally left blank

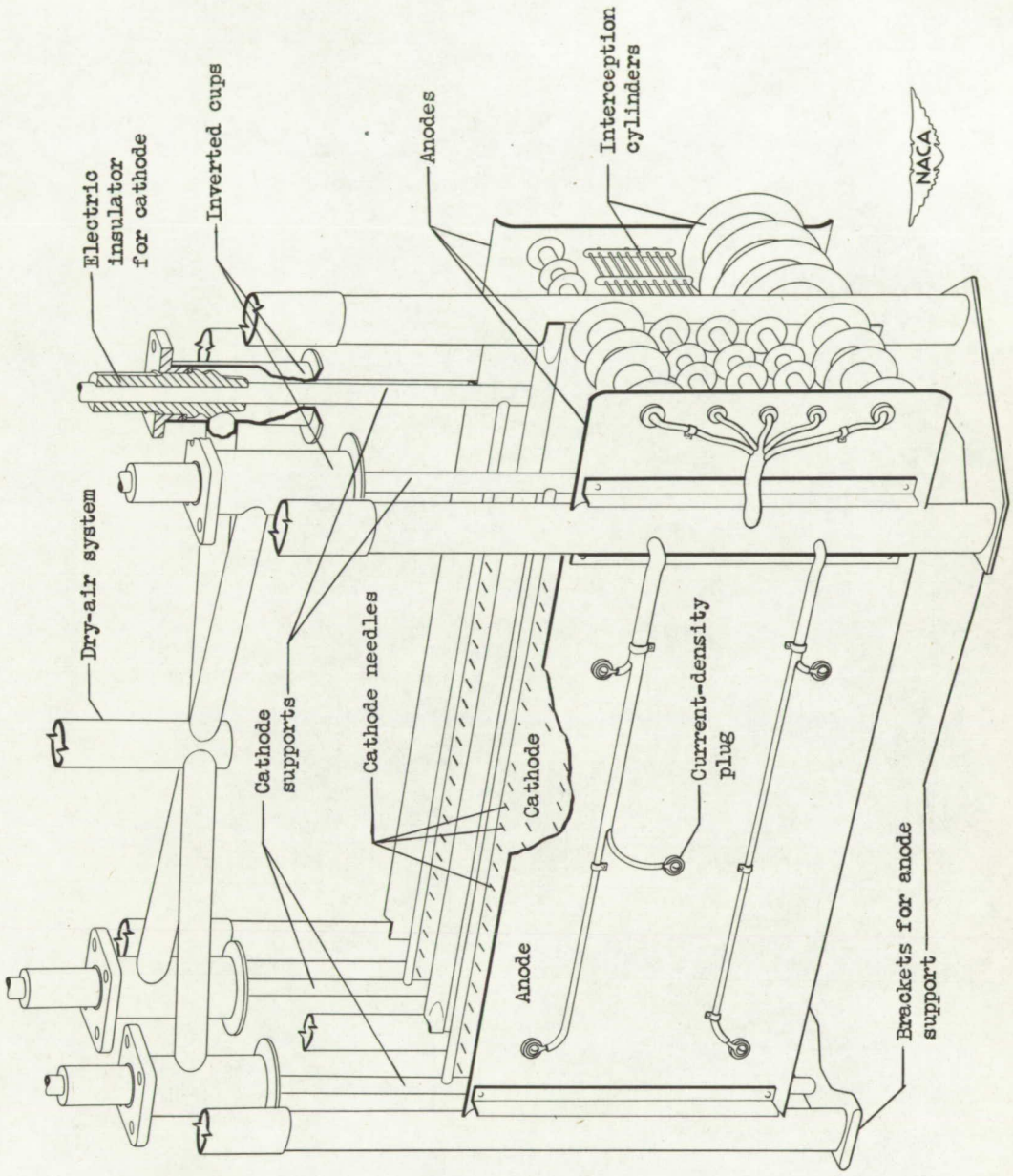

Figure 6. - Schematic diagram of charged-droplet cloud analyzer.

Page intentionally left blank

Page intentionally left blank

Figure 7. - Rear view of charged-droplet cloud analyzer mounted on bomb-bay doors of airplane.

Page intentionally left blank

Page intentionally left blank

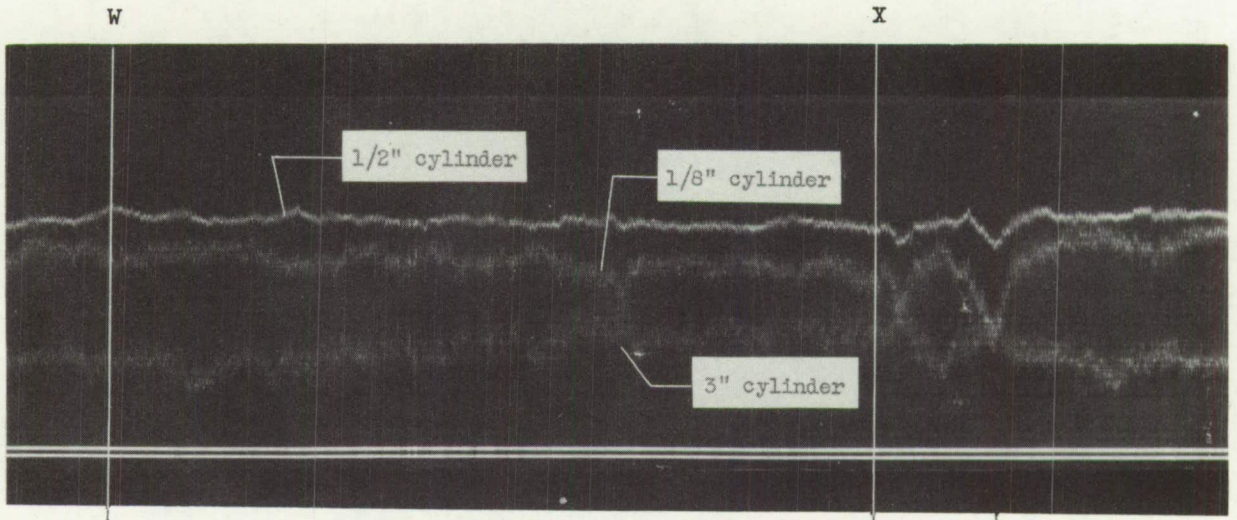

Liquid-water content, grams/cu m	0.3	0.9
Volume-medium droplet diameter, microns	11	8
Distribution	B	C to D

Figure 8. - Flight record through stratocumulus clouds. Trace of fourth cylinder too faint to reproduce in this figure. For the 1/8-inch and 1/2-inch cylinders an increase in current is measured downward whereas for the 3-inch cylinder an increase in current is measured upward.

Page intentionally left blank

Page intentionally left blank

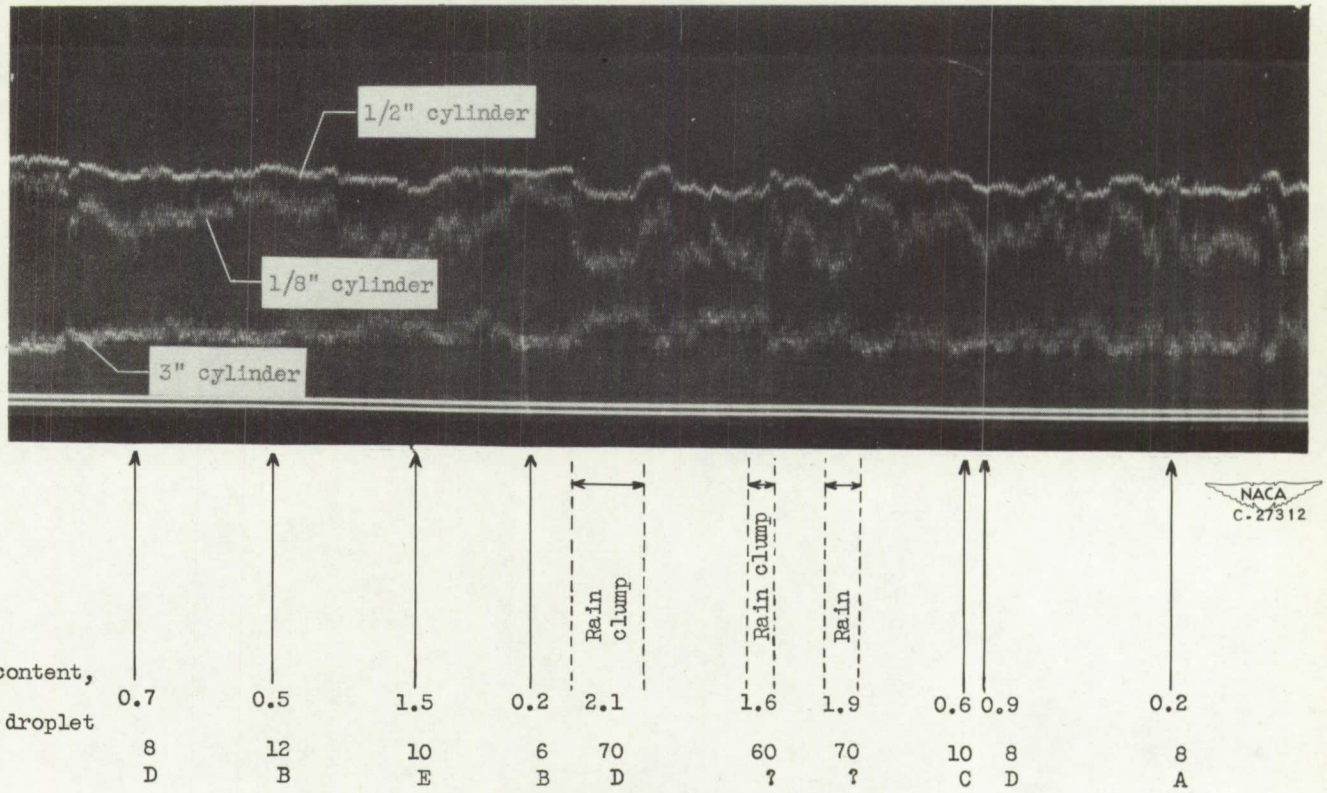

Liquid-water content, grams/cu m	0.7	0.5	1.5	0.2	2.1	1.6	1.9	0.6	0.9	0.2
Volume-medium droplet diameter	8	12	10	6	70	60	70	10	8	8
Distribution	D	B	E	B	D	?	?	C	D	A

Figure 9. - Flight record through stratocumulus cloud congested with clumps of precipitation. Trace of fourth cylinder too faint to reproduce in this figure. For the 1/8-inch and 1/2-inch cylinders an increase in current is measured downward whereas for the 3-inch cylinder an increase in current is measured upward.

Page intentionally left blank

Page intentionally left blank

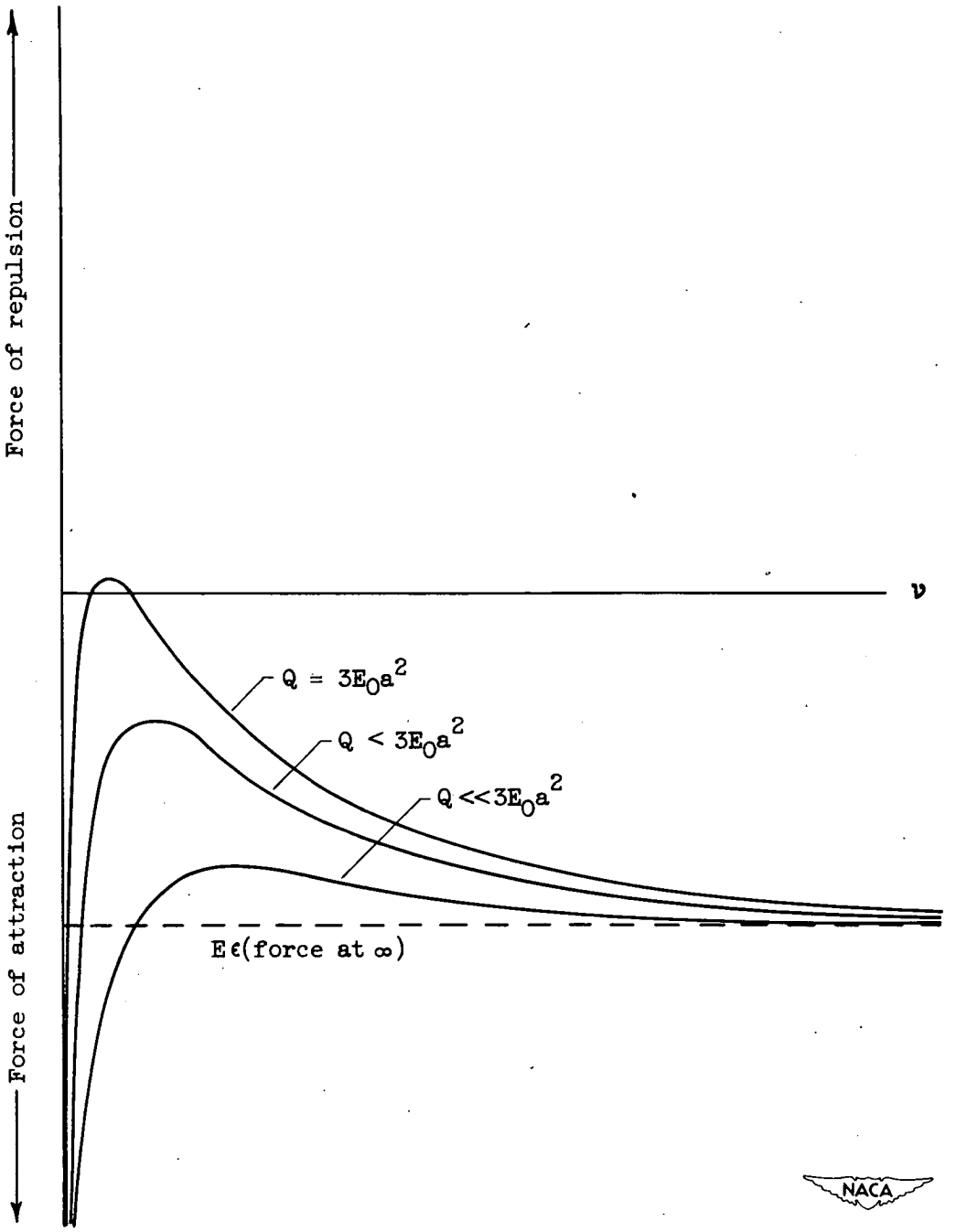

Figure 10. - Force experienced by electrons approaching charged spherical droplet along x-axis for several values of Q.

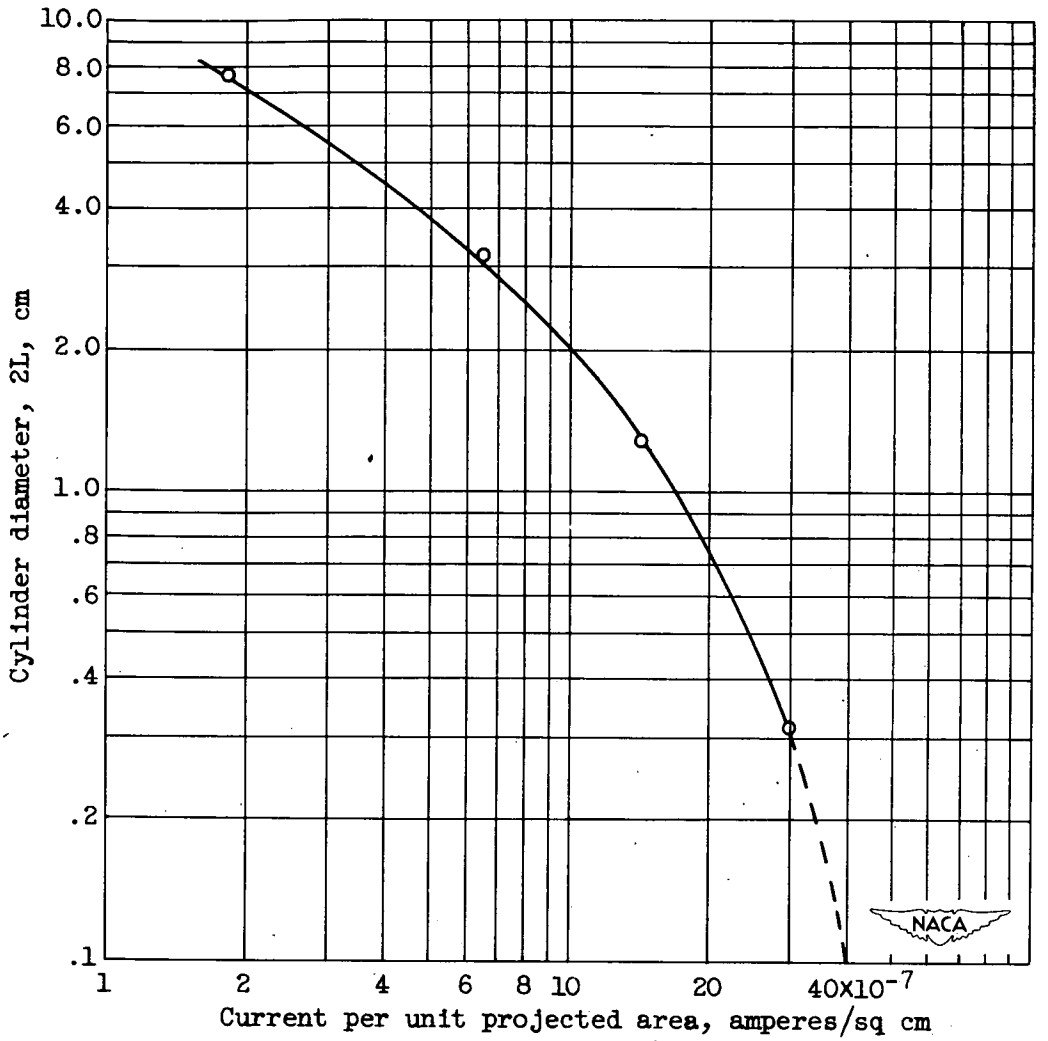

Figure 11. - Electric current measured from cylinders of different size in cumulus cloud. Airplane speed, 200 miles per hour; altitude, 6000 feet.

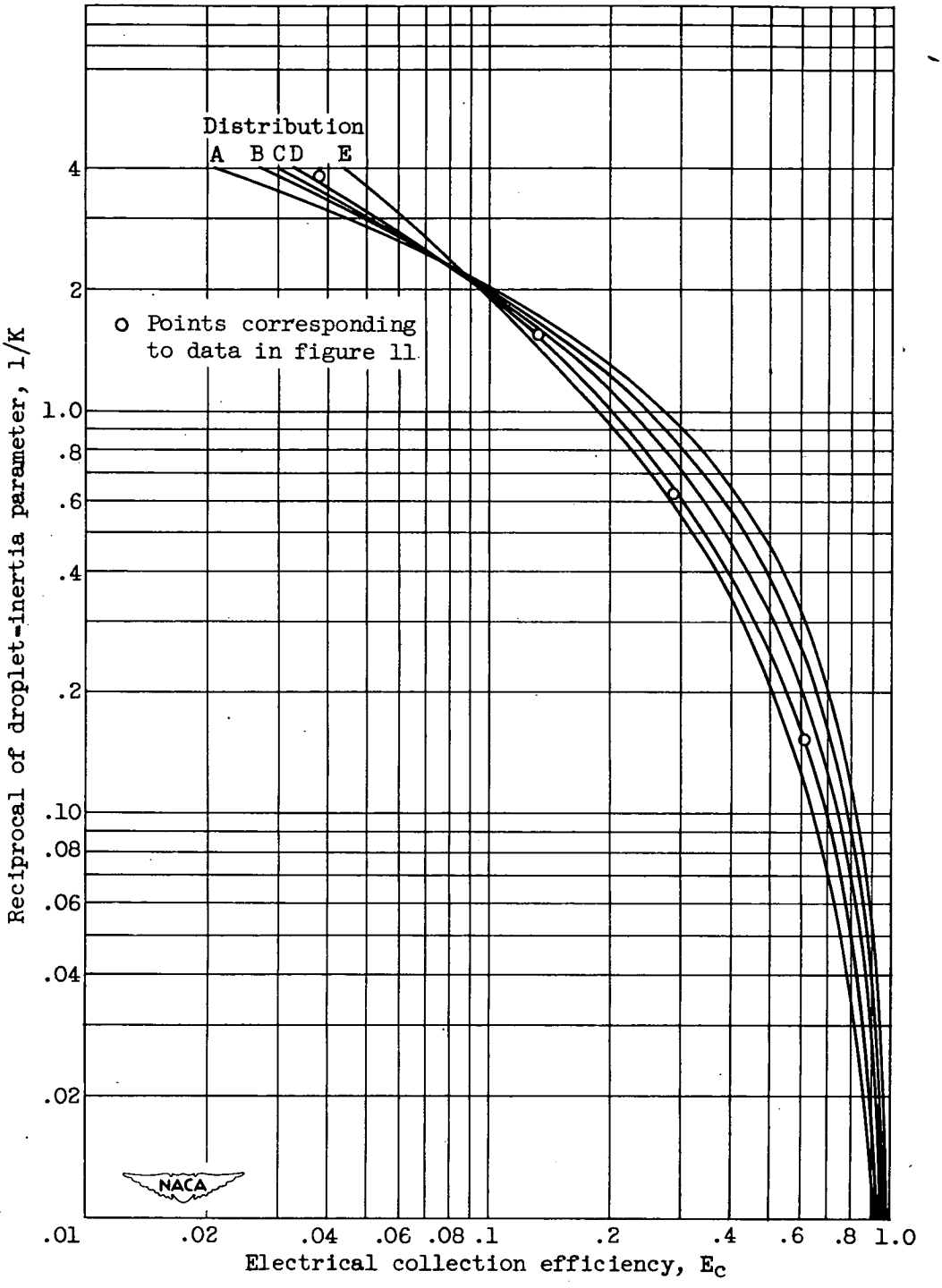

Figure 12. - Droplet-inertia parameter as function of electrical collection efficiency. KΦ, 200; 1/K for volume-median droplet, 4.0.

NACA-Langley - 9-7-51 - 1000